Parameter Extraction through Joint Optimization of Modulation Response and RIN Spectra

Alirio Melgar, Varghese A. Thomas, Justin Lavrencik, Stephen E. Ralph
School of Electrical and Computer Engineering, Georgia Institute of Technology, Atlanta, GA 30332 USA
stephen.ralph@ece.gatech.edu

Abstract: Extraction of VCSEL rate equation model parameters through joint optimization of modulation response and RIN spectra is presented. It accurately accounts for both ISI and noise, and employs drive-dependent parasitics found in VCSELs.

1. Introduction

VCSEL-MMF links have helped achieve high-speed in short reach data center links. Rate equation based modelling [1] and the associated parameter extraction have been studied in the past [2,3]. However, these techniques usually rely on matching only the modulation response of the VCSEL at a few bias points. In this paper, we present a parameter extraction technique capable of accurately estimating laser parameters used to simulate both relative intensity noise (RIN) spectra and small signal modulation response (S_{21}) using stochastic differential laser rate equations. This technique requires only the measured RIN spectra and modulation response of the VCSEL. Our model includes the variation of bias dependent parasitics and the addition of RIN by incorporating Langevin noise sources into the rate equation. Though both RIN and S_{21} measurements are strongly recommended inputs, our model is capable of extracting parameters even when only one type of measurement is available.

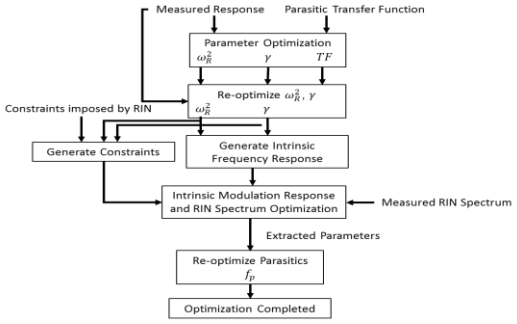

Fig. 1. Parameter Extraction Block Diagram

TABLE I: VCSEL Properties

Description	VCSEL A [4]	VCSEL B [5]	VCSEL C
Injection Efficiency, η_i	0.57	0.81	0.26
Spontaneous Emission Factor, β	$1x10^{-4}$	$1x10^{-3}$	$2.1x10^{-2}$
Carrier Lifetime (ns), τ_n	5	2.12	0.99
Photon Lifetime (ps), τ_p	4.09	5.13	3.02
Gain (s^{-1}), G_o	$10.31x10^5$	$3.69x10^5$	$11.9x10^5$
Gain Saturation Factor, ϵ	$4.18x10^{-6}$	$0.11x10^{-6}$	$2.81x10^{-6}$
Carrier Transparency, N_o	$1x10^5$	$1.96x10^4$	$1.7x10^4$
Carrier Rate Equation	$\frac{dN}{dt}=\frac{\eta_i(I-I_{off})}{q}-\frac{N}{\tau_n}-\frac{G_o(N-N_o)S}{1+\epsilon S}+F_N(t)$		
Photon Rate Equation	$\frac{dS}{dt}=-\frac{S}{\tau_p}+\frac{\beta N}{\tau_n}+\frac{G_o(N-N_o)S}{1+\epsilon S}+F_P(t)$		

2. Parameter Extraction - Frequency Response

Figure 1 details the steps in extracting the VCSEL's rate equation parameters shown in Table 1. For simplicity, a single mode VCSEL model was employed [1], where its rate equation is shown in Table 1. To speed up optimization we must first linearize the rate equations using the differential analysis approach discussed in [6]. The intrinsic response, characterized by the resonance frequency ω_r and damping γ, is given by:

$$H_{laser}(\omega)=\frac{\omega_R^2}{\omega_R^2-\omega^2+j\gamma\omega} \qquad \omega_R^2\approx\frac{S}{\tau_p}\frac{G_o}{1+\epsilon S} \qquad \gamma=4\pi^2\tau_p\left[1+\frac{\epsilon N}{1+\epsilon S}\right]f_R^2+\frac{1}{\tau_n}+\frac{\beta N}{\tau_n S} \tag{1}$$

It is important to note that the laser parameters that make up ω_R^2 and γ in (1) are unique to the rate equation in [1] and must be recalculated if another laser rate equation is used. Note that we have defined (1) as the intrinsic response of the laser which does not account for any internal or external VCSEL parasitics. VCSELs have also been found to exhibit a 3rd order or higher frequency response [7] that cannot be captured by the VCSEL rate equations alone. Therefore, we must introduce parasitics like those found in [8,9]. The contribution of the parasitics can be found from measured data as shown in [2,9] or through a more direct approach as shown in [5, 6]. We choose the direct approach which allows us to write the complete small signal response of the system, which includes the parasitic transfer function $H_{parasitic}(\omega)$ as:

$$H_{total}(\omega)=H_{laser}(\omega)H_{parasitic}(\omega) \qquad H_{parasitic}(\omega)=\frac{\omega_p}{\omega_p+j\omega} \tag{2}$$

Where $H_{parasitic}(\omega)$ has been defined as a simple lowpass filter. More complex parasitic circuits can be chosen [6], on a case-by-case basis, depending on the experimental setup.

3. Parameter Extraction - RIN Spectrum

Two major sources of BER degradation is noise and inter symbol interference (ISI). While optimization of the frequency response ensures an accurate incorporation of ISI, the noise sources also need to be realistically added. RIN is a crucial noise source in a VCSEL-MMF links because it ultimately places an upper limit on the achievable signal to noise ratio. The IEEE 802.3 standard assumes RIN to be white with an equivalent RIN parameter. However, the use of higher baud rates makes the generation of colored RIN crucial, especially when using higher order modulation formats. Noise has been added to the model through the addition of Langevin sources to the carriers and photons [6] where correlations are given by:

$$\langle F_S F_S \rangle = \frac{S}{\tau_P} + 2\frac{\beta NS}{\tau_N} + \frac{\beta N}{\tau_N} - \frac{G_o(N-N_o)}{1+\epsilon S}S \qquad \langle F_N F_N \rangle = 2\frac{\beta NS}{\tau_N} + \frac{\beta N}{\tau_N} - \frac{G_o(N-N_o)}{1+\epsilon S}S + \frac{\eta_i(I+I_{off})}{q} \tag{3}$$

$$\langle F_S F_N \rangle = -\left(2\frac{\beta NS}{\tau_N} + \frac{\beta N}{\tau_N} - \frac{G_o(N-N_o)}{1+\epsilon S}S\right) \tag{4}$$

The photon spectral density and RIN can be expressed as:

$$S_{N_P}(\omega) = \frac{|H(\omega)|^2}{\omega_R^4}[(\gamma_{NN}^2+\omega^2)\langle F_S F_S\rangle + 2\gamma_{NN}\gamma_{SN}\langle F_S F_N\rangle + \gamma_{SN}^2\langle F_N F_N\rangle] \qquad RIN\left(\frac{dB}{Hz}\right) = 10\log_{10}\left(2\frac{S_{N_P}(\omega)}{S^2}\right) \tag{5}$$

where the parameters γ_{NN}, and γ_{SN} are derived using the methodology in [6]. Though the spectral shape of RIN is related to the frequency response of the laser, it is not identical. Hence, optimizing the modulation response does not automatically optimize the RIN spectra of the model. Parameter extraction through joint optimization of the frequency response and the RIN spectra must be performed to have an accurate representation of both. It is important to note that (5) is not the standard definition of RIN, but since the number of photons is directly proportional to output power, it is a good approximation for non-shot noise limited systems.

4. Parameter Extraction Methodology

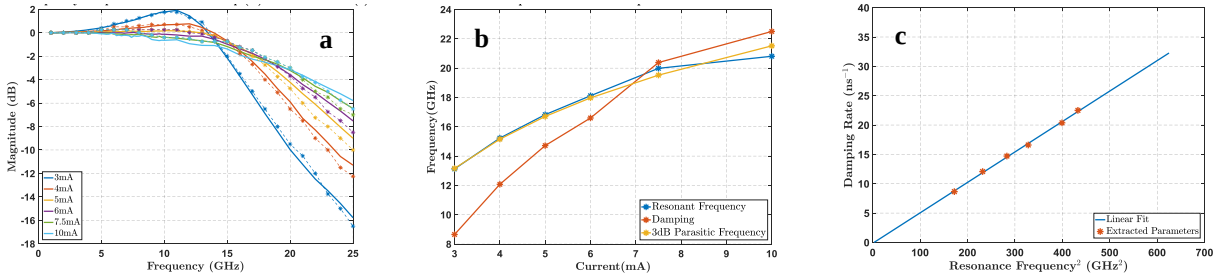

Fig. 2. (a) Matching VCSEL A's frequency response (*) with VCSEL rate equation parameters (-) using parasitic filter extracted from optimization. The extracted rate equation parameters together with the extracted parasitic filter provide a good match between the modelled and measured frequency responses. (b) Optimized current dependent sources. (c) Linear fit of γ with ω_R^2 after fine tuning.

Since no a priori knowledge of the VCSEL is assumed, it is important to develop an iterative approach that will extract a realistic set of laser parameters, and converge to the measured S_{21} and RIN spectrum without the need for time intensive computations. We have developed a multistage extraction process where we match the experimental measurements to our analytical calculations using (1) and (2) which are then used to extract laser parameters. These parameters will be used to match the VCSEL rate equations back with the experimentally measured data. To calculate S_{21} we send tones through the rate equation and measure the frequency response. To calculate RIN we measure the PSD of an unmodulated signal. This split step approach enables us to use mathematical expressions for generating most of our simulated curves during the optimization stage rather than directly integrating the laser rate equations, which significantly reduces the computation time. As shown in Fig. 1a, we first match the analytical expression in (2) to the experimentally measured frequency response by minimizing the mean squared error between (2) and the measured S_{21}. Note that each bias dependent frequency response is optimized independently and in the order of increasing drive current, making sure that the extracted parasitic frequency ω_p increases with the input drive current. After this step we should have full knowledge of ω_R, γ and ω_p for each bias current, as shown in the Fig. 2b. The intrinsic laser response can now be calculated using (1), ω_R, and γ while $H_{parasitic}(\omega)$ in (2) can be used to filter the input current coming into the VCSEL. The damping factor, k, can be extracted by linearizing the damping as shown in Fig. 2c, through the equation $\gamma = kf_R^2 + \gamma_0$, where γ_0 is the damping offset.

Since we have full knowledge of the intrinsic frequency response and RIN spectra of the VCSEL we are now able to expand (1) into its laser parameters. Our cost function maps the intrinsic frequency response and RIN spectra to the

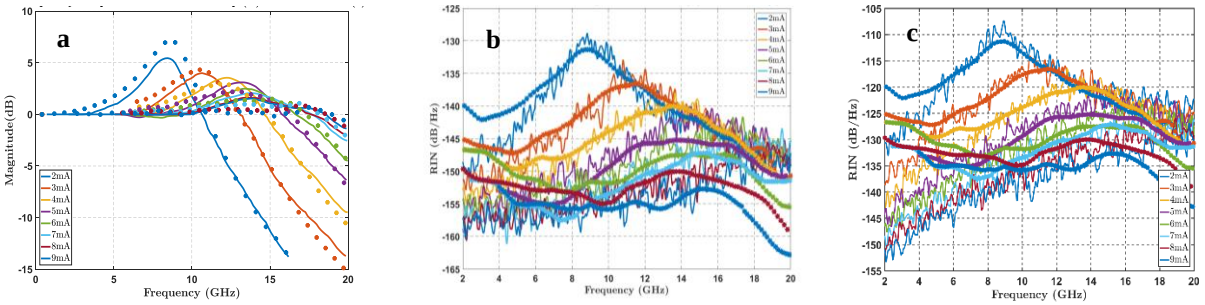

Fig. 3. (a) Matching VCSEL B's measured frequency response (-) with VCSEL rate equation parameters (*) using parasitic filter extracted from optimization. Results show excellent agreement over a wide range of bias points. (b) VCSEL rate equation RIN spectra (-) using parameters shown in Table 1 and measured data from VCSEL B (*). (c) Shifted up version of data from VCSEL B, parameters shown under VCSEL C

individual laser parameters by accounting for all bias points and frequencies that have been experimentally measured, adding their mean squared errors and returning a single error value that is then minimized. A set of reasonable start values has been created and reasonable bounds are assumed for the laser parameters. Twenty-five random starting sets of laser parameters are generated and iteratively optimized, where the set of values with the lowest associated cost is considered a near global minimum solution. Once the laser rate parameters are extracted, the final simulated RIN spectrum and the simulated intrinsic frequency response is generated directly from the laser rate equations. Note that the S_{21} is computed from the laser rate equations by using sinusoidal tones as the input while the RIN spectrum is computed by taking the PSD of the non-modulated output over its mean.

5. Validation

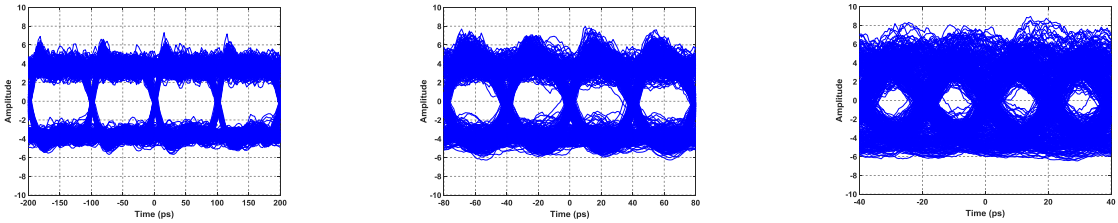

Fig. 4. Stochastic VCSEL rate equation solution to a (a)10G PRBS7 pattern, (b)25G PRBS7 pattern, (c)50G PRBS7 pattern

The extraction method was applied on 3 different VCSELs. Figures 2a and 3a show excellent agreement between simulated and measured values for both VCSELs. Deviations from the measured values can be attributed to both experimental uncertainty and the simplistic view of the parasitics in (2). Figure 3b shows excellent agreement between simulated and experimentally measured RIN. It should be noted that the experimental RIN is higher at lower frequencies due to mode partition noise (MPN) which has not been accounted for in this model. Frequencies above 16GHz also do not match due to the hardware limitations as noted here [5]. To easily view the bias dependent RIN in an eye diagram, the measured RIN data from [5] was artificially shifted up by 20dB as shown in Fig 3c. The S_{21} and RIN spectrum shape the stayed the same and the parameter extraction optimization ran once more. Figure 4 includes the simulated VCSEL RIN, results shown under VCSEL C in Table I. ISI effects become evident as the VCSEL is driven faster. The intensity noise is relative to the optical power level and hence, for the same RIN parameter, there should be more noise added to the higher levels. Most models simply add a constant average noise to the entire signal. However, as seen from Fig. 4 our model adds level-dependent noise.

6. Conclusion

A novel efficient method of extracting parameters for a rate equation based VCSEL model with RIN was presented. It employed joint computations of both modulation bandwidth and RIN spectrum and could accurately extract data from two different manufacturers. The results of the rate equation based model relying on these extracted parameters was found to be in close agreement with experimentally measured results.

7. References

[1] P. V. Mena et al., "A simple rate-equation-based thermal VCSEL model," in JLT, vol. 17, no. 5, pp. 865-872, May 1999.
[2] J. C. Cartledge et al., "Extraction of DFB laser rate equation parameters for system simulation purposes," in JLT, vol. 15, no. 5, pp. 852-860, May 1997.
[3] M. Bruensteiner et al., "Extraction of VCSEL rate-equation parameters for low-bias system simulation," in Quantum Elec., vol. 5, no. 3,1999.
[4] L. M. Giovane et al., "Volume manufacturable high speed 850nm VCSEL for 100G ethernet and beyond," 2016 (OFC), Anaheim, CA, 2016.
[5] S.E. Hashemi, RIN in High-Speed VCSELs for Short Reach Communication, Thesis, Chalmers University of Technology, 2012, pp.41.
[6] L. A. Coldren and S. W. Corzine, Diode lasers and photonics integrated circuits, John Wiley&Sons, New York, USA, 1995, chp.5.
[7] J Lavrencik et al., "DSP-Enabled 100 Gb/s PAM-4 VCSEL MMF Links," J. Lightwave Technol. 35, 3189-3196, 2017.
[8] K Minoglou et al., "A Compact Nonlinear Equivalent Circuit Model and Parameter Extraction Method for Packaged High-Speed VCSELs," JLT 2004.
[9] P. A. Morton et al., "Frequency response subtraction for simple measurement of intrinsic laser dynamic properties" IEEE P.T.L. 1992.